NMR Imaging of Coatings on Porous Substrates

S. J. F. Erich, O. C. G. Adan, L. Pel,* H. P. Huinink, and K. Kopinga

Department of Applied Physics, Eindhoven University of Technology, P.O. Box 513, 5600 MB Eindhoven, The Netherlands

Received March 30, 2006. Revised Manuscript Received June 6, 2006

Coatings are often applied on porous substrates, for example, wood, stone, or gypsum layers. The type and porosity of the substrate influences the coating performance. Until recently, no techniques were available to monitor the drying process in-depth as a function of time with a high spatial resolution (about 5 μm) in nontransparent coating systems. In the study presented in this paper, we show that with high resolution NMR imaging the drying process, consisting of penetration and evaporation of solvent and subsequent curing (chemical cross-linking) on and inside the substrate (wood and gypsum), can be monitored. The drying of a waterborne alkyd emulsion on a gypsum substrate was investigated. The curing of the emulsion was studied for both glass and gypsum substrates as a function of catalyst concentration, in this case cobalt based. Curing was not only observed at the coating surface, but also, in the case of gypsum, it was observed at the coating/substrate interface. On both substrates a concentration dependence of the catalyst concentration was observed. On the gypsum substrate the speed of the observed curing front was always higher than on glass. This indicates that part of the Ca^{2+} ions originating from the gypsum might act as a secondary drier after migration to the coating. The drying of a commercially available solvent-borne alkyd coating was monitored on gypsum and pine wood. The measurements showed that the coating completely penetrates the substrate and starts to cure inside. The results stress that to optimize the coating performance one should explicitly take the substrate into account.

1. Introduction

One example of a type of paint, which is often applied on porous substrates, is alkyd paint. When an alkyd paint is applied onto a porous substrate three drying stages can be distinguished. First, the solvent and/or the resin penetrates the substrate. During the second stage, the solvent evaporates from the coating and the underlying substrate. During the third stage, the coating starts to solidify by the formation of chemical cross-links (curing). Immediately after application the coating penetrates the substrate. When the penetration into the substrate is higher, the adhesion of the coating onto the substrate is likely to increase.[1,2] The depth of penetration depends on the paint properties such as the viscosity and the surface tension and substrate properties such as permeability and characteristic pore sizes. Note that the conductance of flow in porous media is determined by the ratio between the permeability and the viscosity. The driving force is the capillary force, which is proportional to the ratio between the surface tension and the pore size. The flow properties of the three different types of alkyd paint (solvent-borne, high-solid, waterborne) differ, because of differences in viscosity.[3,4]

Many waterborne coatings consist of emulsified resin droplets in water. When these emulsions are applied on a porous substrate the penetration of the different phases in a porous substrate can differ.[5] The size and viscoelastic deformation of the emulsion droplets together with the pore size of the substrate determines whether the resin will enter the substrate. It was suggested by Ostberg et al.[5] that the water phase penetrates deeper into wood than the alkyd resin, because of the high molecular weight of the resin. The difference in penetration behavior of the water and resin phase will have consequences for the additives present inside the coating, such as driers, anti-fungal agents, and pigments. Additives that are partly present in the water phase might end up inside the substrate instead of in the coating, which can have a negative influence on the drying process and many other properties. An important class of additives are the driers. Driers enhance the drying process of alkyd coatings. Their main purpose is to catalyze the oxidative curing process. The most commonly used catalysts for the curing of alkyd resins are cobalt based. During the penetration of the coating into the substrate also part of the catalyst might be transported into the substrate. As a result the concentration in the coating drops, thereby affecting the curing of the coating, which might affect other properties, such as the resistivity against moisture.[6−8]

To study the effects of the substrate on the drying behavior, information on the dynamics of the drying process of the alkyd coating on a porous substrate as a function of depth is required. Except for NMR there are no techniques to follow

* To whom correspondence should be addressed. E-mail: l.pel@tue.nl.

(1) de Meijer, M.; Militz, H. *Holz Roh- Werkst.* **2000**, *58*, 354−362.
(2) Bardage, S. L.; Bjurman, J. *J. Coat. Technol.* **1998**, *70*, 39−47.
(3) Nussbaum, R. M. *Holz Roh- Werkst.* **1994**, *52*, 389−393.
(4) Nussbaum, R. M.; Sutcliffe, E. J.; Hellgren, A. C. *J. Coat. Technol.* **1998**, *70*, 49−57.
(5) Ostberg, G.; Bergenstahl, B.; Sorenssen, K. *J. Coat. Technol.* **1992**, *64*, 33−43.
(6) Thomas, N. L. *Prog. Org. Coat.* **1991**, *19*, 101−121.
(7) van der Wel, G. K.; Adan, O. C. G. *Prog. Org. Coat.* **1999**, *37*, 1−14.
(8) de Meijer, M.; Militz, H. *Holz Roh- Werkst.* **2001**, *58*, 467−475.

10.1021/cm060744x CCC: $33.50
Published on Web 08/04/2006

the drying process as a function of depth in nontransparent coating systems. By using a high resolution NMR imaging setup in combination with additional techniques in a previous study, like Confocal Raman Microscopy, and mass measurements, we were able to distinguish the physical and chemical drying (curing) stage of alkyd coatings in our NMR measurements.[9] When cobalt was used as a catalyst a curing front was observed which was the result of oxygen diffusion limitation and the rate of high chemical reactions.[10] In case of an alternative catalyst based on manganese the curing was observed to be more homogeneous.[11] In this study, we use such a NMR setup to investigate the curing process of alkyd coatings on porous substrates as a function of depth and time. Two types of alkyds are investigated: solvent-borne and a waterborne. The waterborne alkyd coating is applied on nonporous glass, as a reference, and on gypsum which is highly porous. The solvent-borne alkyd coating is applied on gypsum and wood. The depth of penetration, the curing, and the effect of the substrate on the speed of the curing is investigated. In section 2, we briefly discuss the materials and NMR setup used. In section 3 the results of the NMR measurements are presented. This section is subdivided in three parts. First NMR measurements of the waterborne alkyd coating on glass are presented. The catalyst concentration to cure the coatings is varied, and the speed of curing is analyzed. The curing of alkyd on the gypsum substrate is presented in the second part. In the third part, the drying of a solvent-borne alkyd on gypsum and pine wood is studied. Finally, the conclusions are presented in section 4.

2. Experimental Details

2.1. Materials. A waterborne alkyd emulsion, containing approximately 50% water and 50% resin, was used. Nuodex WebCo 8 catalyst was added in different concentrations to catalyze the curing process. The emulsion has an average droplet size of 0.3 μm.[4,12] The glass transition temperature of the un-cross-linked alkyd resin is 2 ± 2 °C. Except for the catalyst no other additives or pigments were added to the emulsion. After the addition of the cobalt catalyst to the emulsion and subsequent mixing, the emulsion was applied on the substrate (nonporous glass or gypsum) using a spiral application rod. The glass substrate used was a 100 μm thick microscope cover glass. The gypsum layer ($CaSO_4 \cdot 2H_2O$) had a thickness of approximately 400 μm and a porosity of about 45%. The layer was made from pure hemihydrate ($CaSO_4 \cdot {}^1/_2H_2O$) using a water to binder mass ratio of 0.66. The average pore diameter of the gypsum was found to be on the order of 1 μm by ref 13, which was calculated from mercury intrusion porosimetry data assuming cylindrical pores. The peak to peak surface roughness was reported to be approximately 5 μm.

Besides the waterborne formulation, a commercially available solvent-borne alkyd was used. This coating was applied on a gypsum substrate approximately 0.3 mm thick and a thin layer of pine wood approximately 0.5 mm thick. For more details on the microscopic structure of pine wood and a microscopic investigation of paint penetrating pine wood, see ref 14.

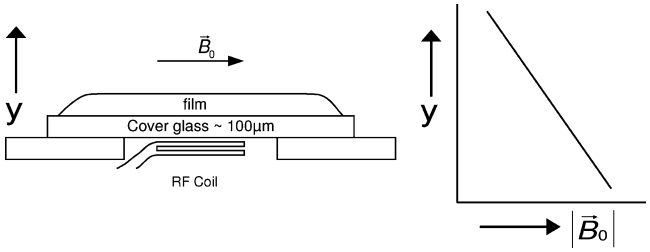

Figure 1. RF coil, film placement, and local magnetic field gradient in the NMR setup.

2.2. NMR Setup. Magnetic resonance imaging (MRI) is a well-known NMR technique for making images of the human body. Its principle is based on the fact that magnetic nuclei located in a magnetic field have a specific resonance frequency and can be excited by a radio frequency (RF) pulse. The resonance frequency f [Hz] depends linearly on the magnitude of the applied magnetic field $\vec{B}$ [T] according to $f = \gamma|\vec{B}|$, where γ [Hz/T] is the gyromagnetic ratio (for hydrogen nuclei, $\gamma = 42.58$ MHz/T). To obtain spatial information the resonance frequency is varied with position according to $f = \gamma(B_0 + G_y y)$, where $G_y = \partial B_z/\partial y$ [T/m] denotes the field gradient in the y direction and B_0 is the magnetic field in the z direction at $y = 0$. To obtain a high spatial resolution (<10 μm) a very high magnetic field gradient should be applied. However, Maxwell's equations show that when a magnetic field gradient in a certain direction is applied, the magnitude of the field $|\vec{B}|$ in a plane perpendicular to that direction and, hence, the resonance frequency are not constant. The corresponding decrease in spatial resolution is very pronounced at high field gradients.

To solve this problem for high magnetic field gradients, the so-called GARField was introduced.[15] In this design a gradient in the magnitude of the magnetic field is realized, $G_y^{\mathrm{mag}} = \mathrm{d}|\vec{B}|/\mathrm{d}y$ (see Figure 1), by using specially shaped magnetic pole tips. It is then possible to distinguish thin layers within a film that is oriented perpendicular to the y direction. The advantage of a setup as shown in Figure 1 is that a sample can be placed directly on top of a surface coil, which gives a good signal-to-noise ratio. Also the gravity acts perpendicular to the applied coating, which makes it possible to measure wet films. Our NMR setup incorporates an electromagnet generating a magnetic field of 1.4 T at the position of the sample. The magnetic field gradient is 36.4 ± 0.2 T/m.

The obtained NMR signals (S) give information not only on the density (concentration) of the magnetic nuclei (spins) ρ, in our case hydrogen nuclei, but also on the mobility of these nuclei. The network structure generated by cross-linking restricts the mobility of the hydrogen atoms connected to the polymer chains. This is reflected in a decrease of the transverse relaxation time T_2 that describes the decay of the NMR signal.

Directly after application of the paint on the substrate, the sample was immediately placed in the NMR setup. The NMR pulse sequence used to obtain the hydrogen density profiles and the signal decay was an Ostroff−Waugh[16] sequence ($90°_x - \tau - [90°_y - \tau - \mathrm{echo} - \tau]_n$). The inter-echo time ($2\tau$) used in the experiments equals 100 μs. The theoretical spatial resolution corresponding to this inter-

(9) Erich, S. J. F.; Laven, J.; Pel, L.; Huinink, H. P.; Kopinga, K. *Prog. Org. Coat.* **2005**, *52*, 210−216.
(10) Erich, S. J. F.; Laven, J.; Pel, L.; Huinink, H. P.; Kopinga, K. *Appl. Phys. Lett.* **2005**, *86*, 134105.
(11) Erich, S. J. F.; Laven, J.; Pel, L.; Huinink, H. P.; Kopinga, K. *Polymer* **2006**, *47*, 1141−1149.
(12) Laven, J.; Uravind, U. K. The Chemical Drying Process in Alkyd Emulsion Paint Films. Presented at Athens Conference on Coatings Science and Technology, Athens, 2003.
(13) Adan, O. C. G. On the fungal defacement of interior finishes. Thesis, Eindhoven University of Technology, Eindhoven, The Netherlands, 1994.
(14) de Meijer, M.; Thurich, K.; Militz, H. *Wood Sci. Technol.* **1998**, *32*, 347−365.
(15) Glover, P. M.; Aptaker, P. S.; Bowler, J. R.; Ciampi, E.; McDonald, P. J. *J. Magn. Reson.* **1999**, *139*, 90−97.
(16) Ostroff, E. D.; Waugh, J. S. *Phys. Rev. Lett.* **1966**, *16*, 1097−1098.

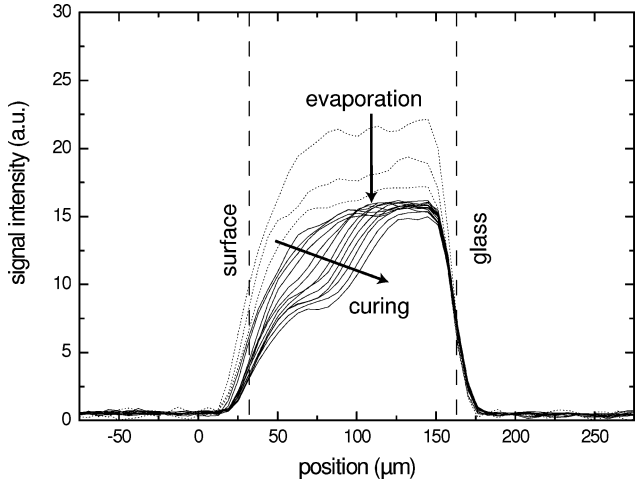

Figure 2. NMR profiles of a coating with 0.007% mass cobalt/mass of the alkyd resin applied on a glass substrate. The profiles are given at $t =$ 0, 1.3, 2.6, 5.2, 7.8, and 10.4 h and then every 13 h. The dotted profiles indicate the evaporation stage, and the solid profiles indicate the curing stage.

echo time setting is 6.6 μm. The acquisition of each profile took about 10 min, using 512 signal averages.

3. Results

3.1. Waterborne Alkyd Applied on Glass. First the drying behavior of the waterborne alkyd emulsion on a glass substrate was investigated. In Figure 2 the NMR profiles are shown for a coating with a cobalt concentration of 0.007% (mass/mass). At the left side of the profiles the surface of the coating is located, and at the right side the glass substrate is located. Directly after application the evaporation stage sets in, represented by the dotted curves. One can see the formation of a cross-linking front: When polymers cross-link and form a network, the mobility of the hydrogen nuclei decreases. As a consequence, the decay rate of the NMR signal increases and part of the signal is lost, which allows the curing to be visualized.[9] The drying behavior was studied for different cobalt catalyst concentrations, ranging from 0.7% (mass/mass) to the alkyd resin to 0.007% (mass/mass).

To characterize the dynamics of the cross-linking front in more detail, we have determined the front positions f from the intersections of the fronts with a line positioned halfway to the height of the front. We will refer to the moment that a front appears and starts to move into the coating as $t = t_0$, which is roughly 2 h after application. The position of the front at $t = t_0$ is denoted by f_0. The front positions f for three typical concentrations (0.7%, 0.07%, and 0.007%) are plotted in Figure 3 as $(f - f_0)^2$ against $t - t_0$. This figure reveals that within experimental inaccuracy the squared front position varies linearly with time. In a previous study it has been shown that oxygen diffusion limits the speed of the cross-linking front and can be described with the following eq 10:

$$f(t) = f_0 + \sqrt{2\nu D\rho_0(t - t_0)} \qquad (1)$$

In this equation f_0 [m] is the front position at the moment t_0 [s] at which the front forms and starts to move into the coating, D [m^2/s] is the diffusion constant of oxygen in the coating, ρ_0 [mol/m^3] is the oxygen density in the surface layer of the coating film, and ν [m^3/mol] is the cross-linked volume per mole of oxygen.

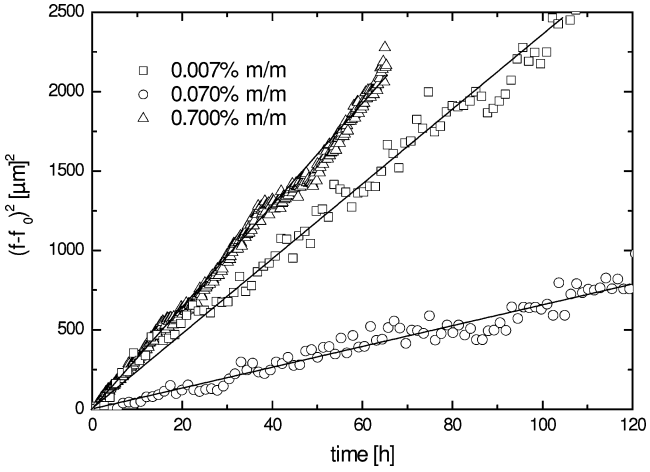

Figure 3. Squared curing front positions of alkyd resins plotted against time for three cobalt catalyst concentrations. The coatings were all applied on a glass substrate. Both the high and the low catalyst concentrations lead to faster curing of the sample.

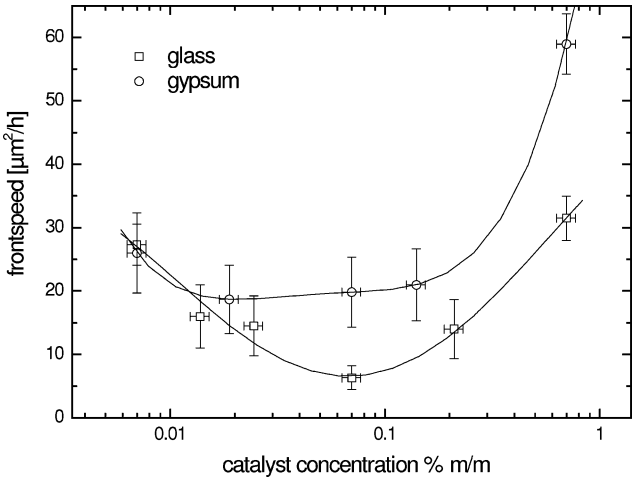

Figure 4. Front speeds of alkyd resins plotted against the catalyst concentration for both the glass and the gypsum substrates.

In Figure 4 the front speed ($2\nu D\rho_0$) is plotted as a function of the catalyst concentration (open squares). The curve through the points is drawn as a guide to the eye. At the lowest and highest concentration the fastest front speeds are observed. The slowest curing occurs at the cobalt concentration of 0.07% (mass/mass), which is a common concentration used in commercial products. According to eq 1 changes in the front speed can be attributed to three variables: ν, D, and ρ_0. It seems that the catalyst concentration influences the final network structure. If the network structure would becomes less dense (higher ν), the diffusion of oxygen increases (higher D), resulting in an increase of the front speed by both variables. This would mean that the highest network density is formed exactly at the Co catalyst concentration of 0.07% (mass/mass).

3.2. Waterborne Alkyd Applied on Gypsum. The waterborne alkyd emulsion was also investigated on the gypsum substrate. The profiles of the NMR measurements are plotted in Figure 5. At the left side the coating is located, and at the right side the gypsum is located. The surface of

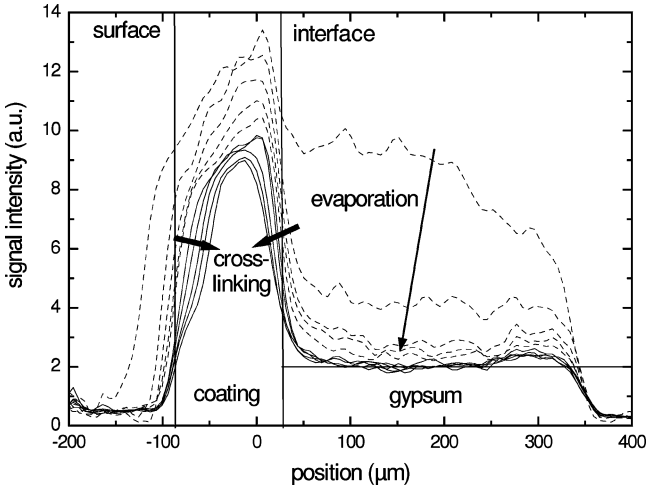

Figure 5. Waterborne alkyd emulsion with 0.07% Co (mass/mass) as a catalyst. The dashed profiles show the penetration and evaporation of the solvent. These profiles are given at $t = 0$, 0.3, 0.6, 1.0, and 1.3 h. The solid profiles show the curing of the coating. These profiles are given at $t = 8$, 16, 49, and 65 h after application. The horizontal line shows the signal from the hydrated gypsum layer, both before and after paint application.

Table 1. Possibility of Penetration of Waterborne Alkyd Emulsion Droplets into a Porous Substrate Based on Droplets Size and Deformability of the Alkyd Droplets, Assuming that the Driving Capillary Forces Are High Enough

size	hard droplets	deformable droplets
droplet > pore	impossible	possible
droplet < pore	possible	possible

the coating and the coating/substrate interface are denoted by the two vertical lines. The measurements show that the penetration of the water phase into the gypsum layer is almost instantaneous and wets the gypsum layer. In practical applications the gypsum substrate is thicker, and as a result the water uptake would be even higher. Directly after this water uptake, the water present in the coating and substrate starts to evaporate. This process is indicated by the dashed profiles in Figure 5. The signal intensities from the gypsum layer before application of the paint and after the evaporation stage are the same. Therefore, it can be concluded that the resin has not penetrated the substrate, except possibly at the interface with a penetration depth smaller than the experimental resolution.

In general, the penetration depth of the resin droplets in the substrate is determined by the deformability of the resin droplets and the size of the alkyd droplets compared to the characteristic pore sizes of the substrate, as was discussed in section 1. Table 1 indicates whether penetration can be expected for a waterborne alkyd emulsion, based on the size of the droplets and the deformability of the droplets, assuming that the driving capillary forces are high enough. If the droplets are difficult to deform but their size is small compared to the pore size, penetration is possible. However, if the droplets are difficult to deform but larger than the pore size, the coating is not expected to penetrate the substrate. In our case the emulsion droplet size (0.3 μm) is comparable to the pore size of the gypsum (approximately 1 μm), and the droplets are difficult to deform (their shape is still visible with atomic force microscopy after drying). Because the internal structure of gypsum is irregular and the pores are not cylindrical, as was assumed in the calculation of the

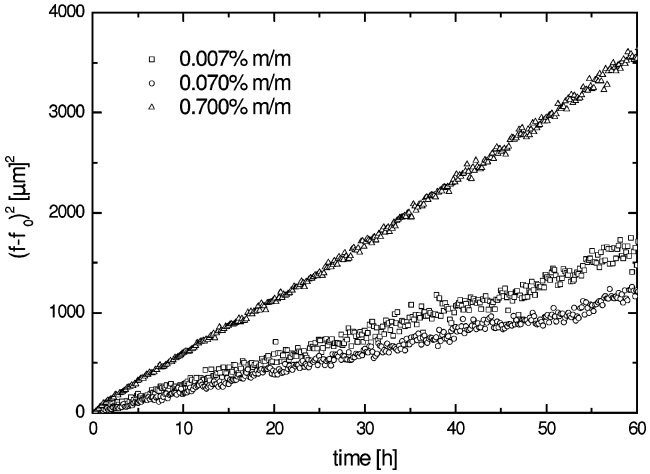

Figure 6. Squared curing front positions observed at the surface of the alkyd coatings applied on a gypsum layer plotted against time for three cobalt catalyst concentrations. Only a high catalyst concentration leads to faster curing of the sample.

porosity of gypsum from mercury intrusion porosimetry,[13] it is likely that the emulsion droplets are still too large to penetrate the substrate. In addition, as a result of the fast absorption of the water phase the resin droplets might already start coalescing before penetrating the substrate.

After the evaporation stage, curing sets in, which is denoted by the two bold arrows in Figure 5. A curing front is visible not only at the surface of the coating but also at the coating/gypsum interface. It is obvious that, at the surface of the coating, the front moves toward the bottom of the coating, whereas at the substrate side the front moves toward the top of the coating. Obviously, oxygen transport is taking place through the gypsum layer, which is possible because it is a porous layer in contact with air.

We have plotted the square of the position of the curing front (at the surface) against time in Figure 6 for three typical catalyst concentrations. Again this figure reveals that within experimental inaccuracy the squared front position varies linearly with time. In Figure 4, the front speeds found for the gypsum substrate are plotted as a function of the cobalt concentration. In general the trend is comparable to that observed for the glass substrate. However, the front speeds observed for the coating on the gypsum layer are always higher than for the same coating applied on glass. Besides this effect, we observe that at higher cobalt concentrations the front speed for the coating on the gypsum layer increases much faster than in the case of the glass substrate.

Transport of cobalt to the substrate cannot explain the observation that the overall front speed is faster on a gypsum substrate. For cobalt concentrations above 0.07% on glass, Figure 4 shows that the front speed increases with cobalt concentration. If part of the catalyst would be transported to the substrate, the concentration and, consequently, the front speed in the coating would decrease. This is not in agreement with the data shown in Figure 4, which clearly indicates a higher front speed when the coating is applied on gypsum instead of glass. However, that part of the cobalt catalyst has been transported out of the coating into the gypsum substrate was confirmed by inductively coupled plasma spectrometry. So another effect is required to explain the

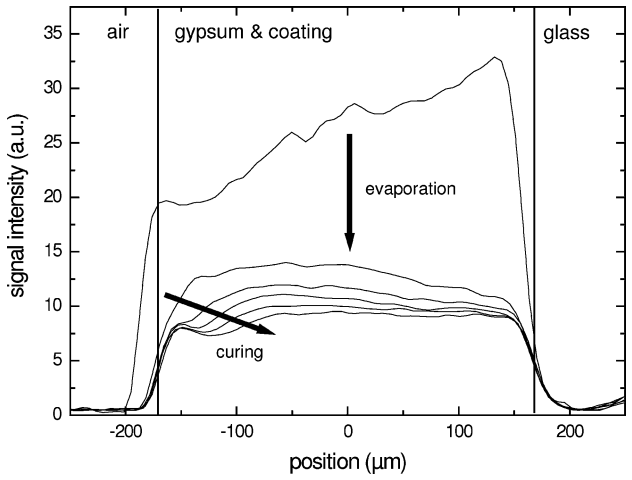

Figure 7. Solvent-borne alkyd coating applied on a gypsum substrate. The NMR profiles are given every 3 h.

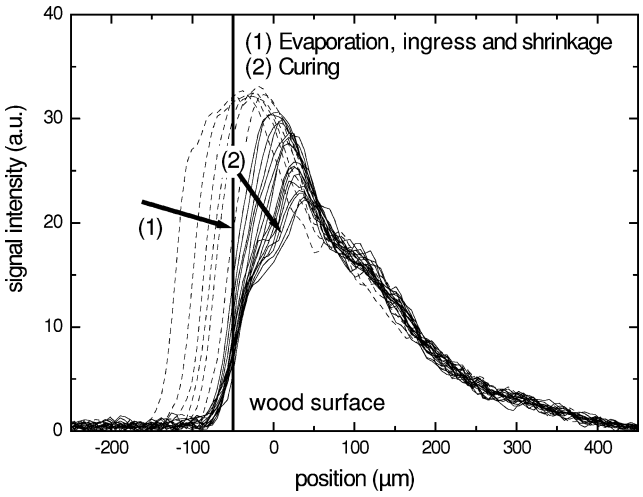

Figure 8. Solvent-borne alkyd coating applied on a wooden substrate. The dashed NMR profiles show the penetration and evaporation of the coating. These profiles are given at $t = 0.3$, 0.6, 1, 1.3, 1.6, and 3.3 h. The solid profiles are given every 1.7 h after the last dashed profile at $t = 3.3$ h. The vertical line indicates the wood surface.

overall increase of front speed. We attribute the increase to the presence of Ca^{2+}. Directly after application the water penetrates the substrate, dissolves some Ca from the gypsum, and via the water Ca^{2+} ions from the $CaSO_4$ might migrate from the substrate into the coating. In a recent study,[17] we have found that addition of Ca/Zr as secondary driers results in an increased front speed, which might indeed explain the observed increased front speed on gypsum substrates.

3.3. Solvent-Borne Alkyd Applied on Gypsum and Wood. This section shows that curing can be investigated even inside a porous substrate. We have studied a solvent-borne alkyd coating on two porous substrates: gypsum and wood. The NMR profiles for the gypsum substrate are plotted in Figure 7. The alkyd completely penetrates the gypsum layer, because it is molecularly dispersed in the solvent and the overall liquid has a low viscosity. In this particular case it is difficult to distinguish the evaporation of the solvent and the curing process. A small curing front is visible, as is indicated in Figure 7 by the arrow at the left. The solvent-borne alkyd was also applied on a thin layer of pine wood with a thickness of approximately 0.5 mm. The results of the measurements are given in Figure 8. The surface of the coating is located at the left side of the profile, and the vertical line shows the surface of the wood. The solvent and resin both penetrate the wood almost instantaneously after application; after the first profile no changes are observed in the deeper region of the wood. In this case the depth of penetration into the wood is approximately equal to the thickness of the pine wood. After the penetration of the substrate the solvent starts to evaporate. This stage is indicated by the dashed profiles in Figure 8. Again a curing front develops, which slowly moves down into the wood.

4. Conclusions

The results presented in this paper have shown that high spatial resolution MRI is an excellent tool to image the dynamical drying processes of alkyd coatings in and on porous substrates. Three drying stages could be visualized: the penetration of the coating in the substrate, the evaporation of the solvent, and the curing.

We have observed that the alkyd resin from the waterborne emulsion remained on top of the gypsum layer, whereas the water phase penetrated into the substrate. For the waterborne alkyd, curing is observed both at the surface of the coating and at the coating/gypsum interface. The speed of the curing front on nonporous glass and on porous gypsum showed a clear dependency on the cobalt concentration. A minimum in the front speed was found for a cobalt concentration of 0.07% Co (mass/mass), which is a commonly used concentration in alkyd coatings. When the coating was applied on a gypsum substrate instead of glass a higher front speed was found. Although a part of the cobalt catalyst was found in the substrate, the faster front speed observed on gypsum cannot be related to the observed higher front speeds. To explain the higher front speeds observed, we suggest that part of the Ca^{2+} ions of the gypsum are transported to the coating during the evaporation stage. This assumption is strengthened by a recent study, showing that the front speed increases when Ca/Zr are added as secondary driers. Further experiments are needed to test this hypothesis, for example, by monitoring the curing speed of waterborne coating on an inert porous substrate, such as glass.

For the solvent-borne alkyd coating the penetration of the coating inside the pine wood substrate was clearly visible, whereas also the curing process could be visualized inside the substrate as a function of depth.

The results unambiguously indicate that to optimize the overall coating performance one should explicitly take the effect of the underlying substrate into account.

Acknowledgment. This research was supported by the Center for Building and Systems TNO-TU/e.

CM060744X

(17) Erich, S. J. F.; ven der Ven, L. G. J.; Huinink, H. P.; Pel, L.; Kopinga, K. *J. Phys. Chem. B* **2006**, *110*, 8166−8170.